Acta Chemica Scandinavica, 1994: 48: 857–860
Printed in Belgium – all rights reserved

ACTA
CHEMICA SCANDINAVICA
ISSN 0904-213X

Short Communication

Crystal Structure and Thermal Stability of Silver Selenite

Pertti Okkonen,[a] Lassi Hiltunen,[a] Markus Koskenlinna[b] and Lauri Niinistö[†,a]

[a]Laboratory of Inorganic and Analytical Chemistry, Helsinki University of Technology, FIN-02150 Espoo, Finland and [b]Technology Development Centre (TEKES), PO Box 69, FIN-00101 Helsinki, Finland

Okkonen, P., Hiltunen, L., Koskenlinna, M. and Niinistö, L., 1994. Crystal Structure and Thermal Stability of Silver Selenite. – Acta Chem. Scand. 48: 857–860 © Acta Chemica Scandinavica 1994.

Silver selenite is formed during recovery of selenium from copper anode slimes when these are subjected to oxidative roasting, whereupon a part of Ag_2Se is converted to Ag_2SeO_3.[1,2] By further thermal treatment in flowing air it is possible to decompose the silver selenite and to completely deselenize the slime pellets.[2] As silver selenite is very sparingly soluble it can also be precipitated from aqueous solutions of silver nitrate and sodium selenite.[3] Ag_2SeO_3 is also the only solid phase formed in the system Ag_2O–SeO_2–H_2O at 100 °C.[4] Moreover, considering the fact that silver selenite is one of the very first metal selenites prepared, it is surprising to find out that its crystal structure has remained unsolved. Therefore a study of Ag_2SeO_3 was undertaken as part of our investigation into the structures and properties of metal selenites.

Experimental

Synthesis. Crystals of Ag_2SeO_3 were grown hydrothermally in a steel vessel lined with teflon where an aqueous solution of $AgNO_3$ (0.1 M) and H_2SeO_3 (0.1 M) in the molar ratio of 1:1 was heated for 2 days at 220 °C. The colorless, needle-shaped crystals were washed with water and ethanol.

Thermal analysis. Thermal behaviour was studied with a Seiko TG/DTA 320 instrument. Sample size was about 15 mg and heating rate was 3 °C min^{-1}. The measurements were carried out in dynamic air and nitrogen atmospheres.

IR spectra. The IR spectrum was recorded with a Nicolet Magna IR spectrometer 750. The KBr and polyethylene pellet techniques were used in the mid-IR and far-IR ranges, respectively.

Crystallographic study. The X-ray diffraction measurements were made with a Syntex $P2_1$ four-circle diffractometer using graphite-monochromatized Mo$K\alpha$ radiation. Unit-cell dimensions were refined from single-crystal data by least-squares calculations. Intensity data were corrected for Lorenz and polarization effects as well as for absorption. Further details of the data collection and structure determination are given in Table 1.

Table 1. Summary of crystal data, intensity collection and structure refinement for Ag_2SeO_3.

Crystal data	
Formula	Ag_2SeO_3
Mol. wt.	342.7
Crystal system	Monoclinic
Space group	$P2_1/c$
a/Å	4.854(1)
b/Å	10.332(3)
c/Å	6.956(2)
β/°	91.13(2)
V/Å^3	348.8
Z	4
d_{calc}/g cm^{-3}	6.526
Radiation	Mo$K\alpha$ (λ = 0.710 69 Å)
μ(Mo$K\alpha$)/mm^{-1}	212.7
Crystal form	Needle-shaped
Crystal size	0.25×0.06×0.03 mm
Data collection and structure refinement	
Data collection	ω-scan
Scan speed/° min^{-1}	1.5–30
No. of data collected	2039
No. of unique data $I_{obs} > 2\sigma(I_{obs})$	1020
Solution	SHELX-86, Patterson method
Abs. correction	Empirical
No. of variables	56
Weighting scheme	$(9.5310/\sigma^2)F$
R ($R=\Sigma\|F_O\| - \|F_c\|/\Sigma\|F_O\|$)	0.0644
R_w ($R_w=[(\Sigma w(\|F_O\| - \|F_c\|)^2/\Sigma wF_O^2)]^{1/2}$)	0.0585
Max. peak in difference map/e$^-$ Å^{-3}	3

† To whom correspondence should be addressed.

Results and discussion

Thermal stability. Whereas earlier thermogravimetric studies had indicated decomposition through disproportionation involving Ag_2Se and Ag_2SeO_4, most reports now agree on a direct degradation into metallic silver and selenium dioxide.[2,5–7] Simultaneous TG/DTG/DTA measurements enabled us to make an unambiguous interpretation of thermal data. Thus, according to the thermoanalytical curves shown in Fig. 1 the thermal processes in air are the following under the experimental conditions chosen:

$$Ag_2SeO_3(s) \rightarrow Ag_2SeO_3(l) \quad (1)$$

$$Ag_2SeO_3(l) \rightarrow 2Ag(s) + SeO_2 + {}^1/_2O_2(g) \quad (2)$$

$$Ag(s) \rightarrow Ag(l) \quad (3)$$

Ag_2SeO_3 melts at 540°C (DTA maximum) almost overlapping with the onset of decomposition, reaction (2). Finally, the melting of silver, reaction (3), is observed in the DTA curve at 950°C. The observed and calculated weight losses in air for the reaction (2) are 37.5 and 37.0%, respectively.

In a nitrogen atmosphere reaction (2) takes place at a slightly lower temperature (the difference in DTG maxima is ca. 10°C) than in air, thus corroborating the oxygen evolution.

IR spectra. The infrared spectrum of Ag_2SeO_3 shows the typical features of a pyramidal SeO_3^{2-} ion, *viz.* vibrations (cm^{-1}) due to the symmetric (818m) and asymmetric (767s) stretch and the corresponding bending modes (436m and 385m, respectively). The weak vibration at 668 cm^{-1} is possibly a combination band. These values deviate slightly from those registered by Rocchiccioli in Nujol mulls.[8]

X-Ray crystallography. Ag_2SeO_3 forms monoclinic crystals with space group $P2_1/c$. The unit-cell data are in agreement with the published powder pattern.[9] The final atomic coordinates are listed in Table 2, while Table 3 gives the bond distances and angles. There are no significant differences in the Se–O distances within the SeO_3^{2-} ion, and the average value 1.70 Å is in agreement with the values found in metal selenites,[10] including the only silver-containing selenite with a known structure,

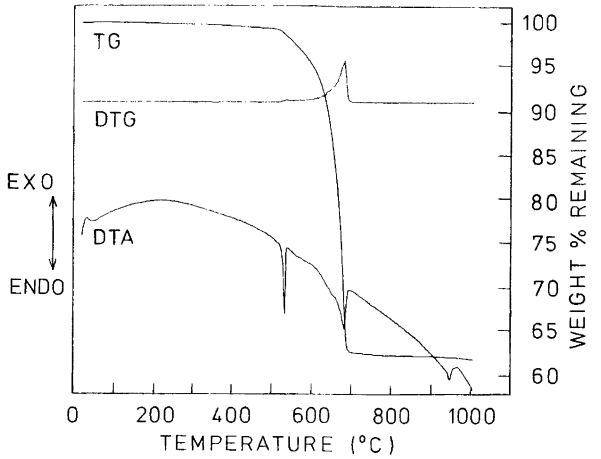

Fig. 1. Simultaneous TG/DTG and DTA curves for the thermal decomposition of Ag_2SeO_3 in flowing air using a heating rate of 3°C min^{-1}. The sample weight is 15.2 mg.

$Ag_5Cu_2(NO_3)(SeO_3)_4$.[11] The angles are within normal ranges, too.

The unit-cell packing is shown in Fig. 2, while Fig. 3 presents the structure from the point of view of the selenite groups. The selenite pyramids run parallel to the *x*-axis, connecting the Ag^+ ions. The oxygens of the selenite group constitute also the oxygens of the two crystallographically different AgO_6 octahedra. The corner-connected arrangement of the two octahedra, $Ag1O_6$ and $Ag2O_6$, is presented in Fig. 4. Whereas the $Ag2O_6$ octahedron is rather regular (Ag–O: 2.46–2.56 Å), Ag1 is surrounded by six oxygens at distances ranging from 2.33 to 2.94 Å (Table 3). The longest distance involves O2, and also the symmetry-related O2 atom at the opposite vertex is relatively far away from Ag1 (2.68 Å), thus leading to a significant elongation of the octahedron as compared to $Ag2O_6$. The $Ag1–O2^2$ distance significantly exceeds the sum of the ionic radii (1.26 + 1.40 Å), however.

Taking into account the space required by the lone electron pair of Se(IV) in the SeO_3^{2-} pyramids, the packing of the SeO_3 and AgO_6 polyhedra can be regarded as rather effective (cf. Figs. 2 and 3). The close packing and the absence of directional covalent bonding leads to a structure in which the oxygens are simultaneously at contact with several Ag^+ ions, for instance O1 has three such distances (Table 2). This can be compared to the

Table 2. Atomic coordinates with isotropic temperature factors for Ag_2SeO_3.

Atom	*x*	*y*	*z*	B^a
Ag1	0.2616(2)	0.2519(1)	0.0916(2)	2.17
Ag2	0.2526(2)	0.5837(1)	0.6357(1)	2.04
Se1	0.7398(3)	0.4083(1)	0.8358(2)	1.35
O1	0.3891(19)	0.3948(8)	0.8505(12)	1.68
O2	0.7623(21)	0.5371(9)	0.6864(14)	2.34
O3	0.7965(20)	0.2871(8)	0.6770(13)	1.77

[a] The isotropic temperature factors were calculated here from the mean square displacements: $B = 8\pi^2 u^2$.

Table 3. Bond distances (in Å) and angles (in °) in Ag_2SeO_3.

Ag1–O1	2.327(9)	Ag2–O2	2.460(10)
Ag1–O3^4	2.380(10)	Ag2–O3^2	2.486(8)
Ag1–O1^3	2.425(9)	Ag2–O1	2.538(9)
Ag1–O2^1	2.675(9)	Ag2–O2^2	2.538(10)
Ag1–O3^5	2.682(10)	Ag2–O3^1	2.559(9)
Ag1–O2^2	2.944(9)	Ag2–O2^1	2.565(10)
Se–O1	1.713(9)	O1–Se–O2	100.2(5)
Se–O2	1.694(9)	O1–Se–O3	98.8(4)
Se–O3	1.696(9)	O2–Se–O3	99.6(4)
O1–Ag1–O1^3	149.8(4)	O1–Ag2–O2	90.4(3)
O1–Ag1–O2^2	90.7(3)	O1–Ag2–O2	62.0(3)
O1–Ag1–O2^1	85.1(3)	O1–Ag2–O2^1	98.2(3)
O1–Ag1–O3^4	123.7(3)	O1–Ag2–O3^2	111.6(3)
O1–Ag1–O3^5	89.1(3)	O1–Ag2–O3^1	157.0(3)
O1^3–Ag1–O2^2	91.3(3)	O2–Ag2–O2	152.4(4)
O1^3–Ag1–O2^1	95.4(3)	O2–Ag2–O2^1	91.1(3)
O1^3–Ag1–O3^4	86.5(3)	O2–Ag2–O3^2	89.3(3)
O1^3–Ag1–O3^5	60.7(3)	O2–Ag2–O3^1	98.6(3)
O2^2–Ag1–O2^1	172.6(4)	O2–Ag2–O2^1	92.3(3)
O2^2–Ag1–O3^4	90.6(3)	O2–Ag2–O3^2	101.0(3)
O2^2–Ag1–O3^5	93.3(3)	O2–Ag2–O3^1	106.9(3)
O2^1–Ag1–O3^4	86.7(3)	O2^1–Ag2–O3^2	150.2(3)
O2^1–Ag1–O3^5	92.7(3)	O2^1–Ag2–O3^1	60.7(3)
O3^3–Ag1–O3^5	146.9(4)	O3^2–Ag2–O3^1	89.8(1)

Symmetry code: none, *x, y, z;* ^{1} *−x, −y, −z;* ^{2} *−x, y−1/2, 1/2−z;* ^{3}*x, 1/2−y, 1/2+z;* ^{4}*x−1, 1/2−y; z−1/2;* ^{5}*x, 1/2−y, z−1/2.*

structure of $Ag_5Cu_2(NO_3)(SeO_3)_4$, where the silver ions are irregularly coordinated; one is linearly bound to two selenite oxygens at 2.38 Å and to four additional ones at 2.90–2.95 Å, while the two other crystallographically independent Ag^+ ions have 6 or 7 contacts ranging from 2.20 to 3.05 Å.[11]

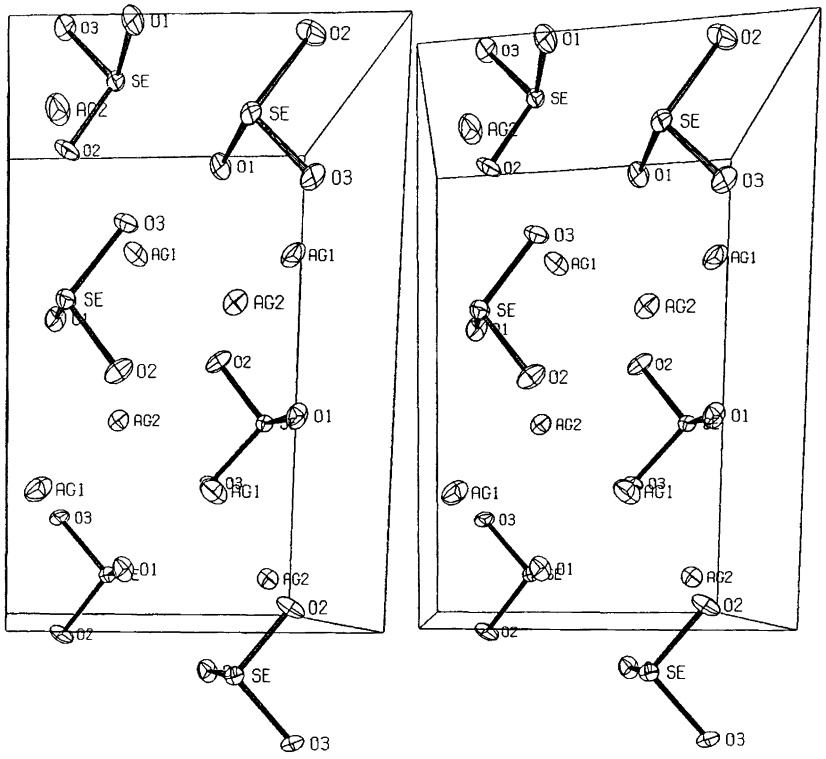

Fig. 2. A stereoscopic view showing the unit cell packing of Ag_2SeO_3. The *b*-axis is vertical and the *a*-axis points into the paper.

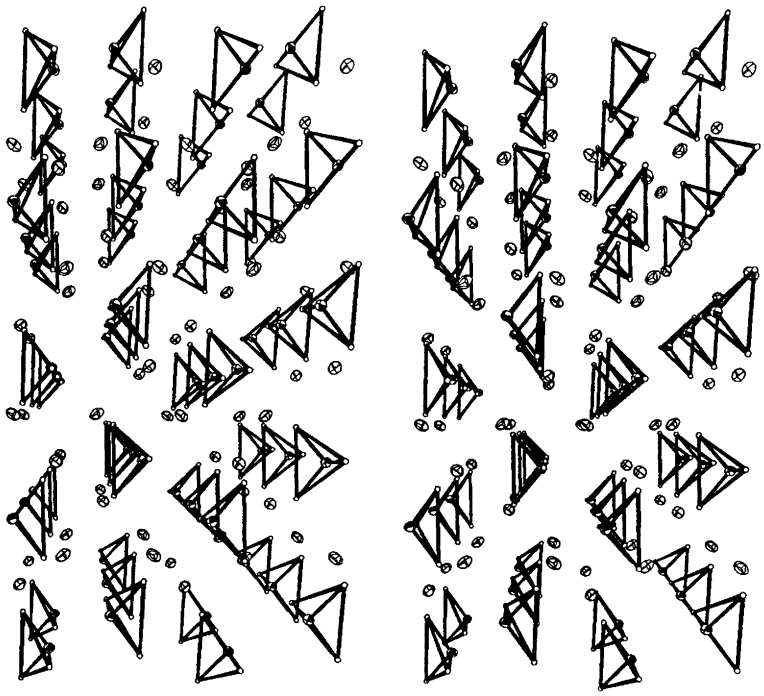

Fig. 3. A stereoscopic view of packing of selenite tetrahedra around silver ions as viewed along the *a*-axis.

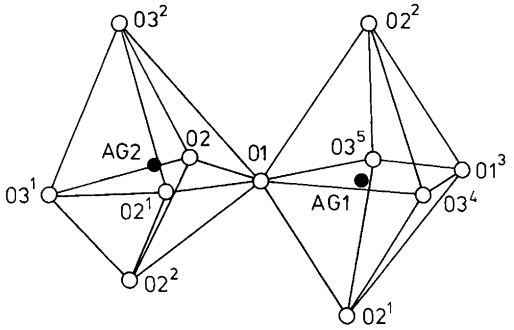

Fig. 4. A schematic view showing the joining of two AgO_6 octahedra. The atomic numbering and symmetry code are as in Table 2.

References

1. Löschau, S. *Freiberger Forschungsh., Teil B 60* (1961) 7.
2. Dutton, W. A., van den Steen, A. J. and Themelis, N. J. *Metallurg. Trans. 2* (1971) 3091.
3. Selivanova, N. M., Leschinskaya, Z. L. and Klushina, T. V. *Zh. Fiz. Khim. 36* (1962) 1349; *Russ. J. Phys. Chem. (Engl. Transl.) 36* (1962) 719.
4. Ojkova, T. and Gospodinov, G. *Z. Anorg. Allg. Chem. 484* (1982) 235.
5. Rocchiccioli, C. *Ann. Chim. (Paris) 13* (1960) 1023.
6. Buketov, E. A., Pashinkin, A. S., Ogorets, M. Z., Muldagalieva, R. A. and Sapozhnikov, R. A. *Zh. Neorg. Khim. 9* (1964) 2701; *Russ. J. Inorg. Chem. (Engl. Transl.) 9* (1964) 1456.
7. Gospodinov, G. C. and Bogdanov, B. G. *Thermochim. Acta 75* (1984) 295.
8. Rocchiccioli, C. *Compt. Rend. 247* (1958) 1108.
9. Joint Committee on Powder Diffraction Standards, Card 34–382.
10. Serezhkina, L. B., Rastsvetaeva, R. K. and Serezhkin, V. N. *Koord. Khim. 16* (1990) 1327; *Coord. Chem. (Engl. Transl.) 16* (1990) 702.
11. Effenberger, H. *Acta Crystallogr., Sect. C 47* (1991) 2522.

Received February 2, 1994.